A HIERARCHICAL PRECONDITIONER FOR THE MORTAR FINITE ELEMENT METHOD

MARIO A. CASARIN* AND OLOF B. WIDLUND†

Abstract. Mortar elements form a family of nonconforming finite element methods that are more flexible than conforming finite elements and are known to be as accurate as their conforming counterparts. A fast iterative method is developed for linear, second order elliptic equations in the plane. Our algorithm is modeled on a hierarchical basis preconditioner previously analyzed and tested, for the conforming case, by Barry Smith and the second author. A complete analysis and results of numerical experiments are given for lower order mortar elements and geometrically conforming decompositions of the region into subregions.

Key words. domain decomposition, mortar finite element method, hierarchical preconditioner

AMS(MOS) subject classifications. 65F30, 65N22, 65N30, 65N55

1. Introduction. Mortar finite element methods were introduced by Bernardi, Maday, and Patera; see [8]. The discretization of an elliptic, second order problem starts by partitioning the computational domain Ω into the union of nonoverlapping subregions (substructures), $\{\Omega_i\}_{i=1}^I$, and an interface Γ, which is the set of points which belong to the boundaries of at least two subregions. In this paper, we restrict ourselves to the geometrically conforming case in two dimensions; the intersection between the closure of two different subregions is either empty, a vertex, or a whole edge. We note that mortar element methods have also been developed for geometrically nonconforming decompositions of the given region, i.e. for decompositions which violate this rule, as well as for problems in three dimensions.

The restriction to any subregion Ω_i of the mortar finite element space considered here, is just a standard piece-wise linear finite element space. We can adopt a strategy of successive refinement to obtain flexible, geometrically conforming, and shape regular triangulations of each of the subregions. The meshes of two neighboring subregions do not necessarily match on their common interface and the elements of the discrete space V^h are typically discontinuous across the interface Γ. Instead of pointwise continuity, the interface jumps are made orthogonal to a carefully chosen space of trial functions. In our work, we exclusively consider the second generation mortar element methods for which continuity is not even imposed at the vertices of the substructures; even if the meshes match across the interface between adjacent subregions, the mortar finite element functions will not, generally, be pointwise continuous.

Similarly as when working with other nonconforming methods, the original bilinear form $a(\cdot,\cdot)$ is replaced by $a^\Gamma(\cdot,\cdot)$ defined as the sum of contributions from the individual

* Courant Institute of Mathematical Sciences, New York University, 251 Mercer Street, New York, N.Y. 10012. Electronic mail address: casarin@cims.nyu.edu. This work has been supported in part by a Brazilian graduate student fellowship from CNPq, in part by the National Science Foundation under Grant NSF-CCR-9503408, and in part by the U. S. Department of Energy under contract DE-FG02-92ER25127.

† Courant Institute of Mathematical Sciences, 251 Mercer St, New York, NY 10012. Electronic mail address: widlund@cs.nyu.edu. This work has been supported in part by the National Science Foundation under Grant NSF-CCR-9503408, and in part by the U. S. Department of Energy under contract DE-FG02-92ER25127.

subregions to $a(\cdot,\cdot)$:

$$a^{\Gamma}(u_h, v_h) = \sum_{i=1}^{I} a_{\Omega_i}(u_h, v_h). \tag{1}$$

For $u_h = v_h$, we obtain the square of what is often called a broken norm. Here the norm has been broken along Γ and it is finite for any element of the mortar space even if it is discontinuous across Γ.

It is known that the resulting discrete variational problem gives rise to a linear system with a symmetric, positive definite matrix, and that its solution is an accurate approximation to the exact solution of the continuous problem; see [4, 5, 8] where error bounds of the same type as for standard conforming methods are derived.

In this paper, we address the issue of solving this linear system efficiently. We note that direct methods and classical, unpreconditioned iterative methods have well-known limitations. Domain decomposition algorithms, which form a special family of preconditioned conjugate gradient methods, have been developed extensively for standard conforming finite elements. The present study is part of an effort to extend the applicability of these methods to a wider family of discretizations. Here, we have chosen to use a hierarchical preconditioner modeled on an algorithm developed by Smith and Widlund [18]. That work, in turn, was based on a result of Yserentant [20]. We note that, in the conforming case, we had found this to be an effective preconditioner with certain advantages over some similar iterative methods because of being relatively simple, and as effective as the others; cf. [17] for motivation and a comparative study.

Our algorithm is a preconditioned conjugate gradient method with a condition number bounded from above by $C(1+\ell)^2$. Here ℓ is the maximum number of successive refinements of any individual subregion Ω_i into elements, and C a constant which depends on the minimal angle of the triangulations into subregions and elements, but which is otherwise independent of ℓ, and the number and size of the substructures and elements. Our method is an iterative substructuring algorithm, i.e. the linear system is first reduced in size by implicitly eliminating all the nodal variables interior to the subregions. The nodal values on $\partial\Omega_N$, the part of the boundary where a Neumann condition is imposed, are also classified as being interior. In each step of the iteration, we solve a local boundary value problem for each subregion, perform very fast local transformations between the nodal and hierarchical bases restricted to each individual edge, and solve a global problem of a dimension equal to the number of crosspoints of the partitioning of the region into substructures. We note that the global coarse space of our algorithm is the same as for the conforming case. This is in contrast with those proposed in Achdou, Maday, and Widlund [3] and Dryja [13], which are of higher dimension.

Other iterative substructuring methods for mortar finite elements have been described and analyzed by Achdou, Kuznetsov, and Pironneau [1, 2] and Le Tallec [15]. Ongoing work in the field also includes Maday and Widlund [16]. We also note that certain technical issues related to extending the algorithm of this paper to higher order elements are discussed in a recent paper by the first author; cf. [11].

In the next section, we introduce the mortar space V^h, and establish some properties of certain special vertex basis functions. In Section 3, we introduce the hierarchical structure, and describe and analyze our algorithm. In Section 4, we report on some numerical experiments that demonstrate the effectiveness of the algorithm in a relatively wide range of situations.

2. The Elliptic Problem and the Mortar Finite Element Method. Let Ω be a bounded polygonal region in $\mathbb{R}^2$ with a diameter on the order of 1. For simplicity, we consider only Poisson's equation as a model problem. The boundary of Ω, $\partial\Omega$, is the union of $\partial\Omega_N$ and $\partial\Omega_D$ on which Neumann and homogeneous Dirichlet conditions are imposed, respectively. We assume that $\partial\Omega_D$ is a closed set of positive measure. Let

$$a(u,v) = \int_\Omega \nabla u \cdot \nabla v \, dx \tag{2}$$

define an elliptic and continuous bilinear form on $H_0^1(\Omega, \partial\Omega_D)$, the subspace of $H^1(\Omega)$ with elements which vanish on $\partial\Omega_D$. Let $f(\cdot)$ be a continuous linear functional on $H_0^1(\Omega, \partial\Omega_D)$; it includes a contribution from the nonhomogeneous Neumann boundary values, if any, in the form of a line integral. Then, by the Lax-Milgram lemma, there is a unique $u \in H_0^1(\Omega, \partial\Omega_D)$ satisfying

$$a(u,v) = f(v) \quad \forall v \in H_0^1(\Omega, \partial\Omega_D). \tag{3}$$

2.1. Triangulation of the region and the subregions. We assume that Ω can be partitioned into nonoverlapping, shape regular triangular substructures, $\{\Omega_i\}_{i=1}^I$; we will focus on the analysis of the case of triangular substructures but we note that a similar theory can be developed for the quadrilateral case. As noted before, the intersection between the closure of any two distinct substructures is either empty, a vertex, or a whole edge; this coarse triangulation is geometrically conforming. We also assume that if $\partial\Omega_i \cap \partial\Omega$ is nonempty, then the boundary condition does not change type in the interior of any edge of Ω_i. We note that we are primarily interested in the case of a large number of subregions, since the potential for parallelizing our method depends on having enough subproblems. Our analysis will only involve individual subregions and their next neighbors. The subregions are assumed to be shape regular but there is no need to assume that the coarse triangulation is quasi-uniform. To simplify our analysis, we assume that the triangulation of each subregion is quasi-uniform. We will denote the diameter of the subregion Ω_i by H_i, and the smallest diameter of any of its elements by h_i. Our results depend only on the minimal angle of the overall triangulation, and ℓ, the maximum of the number of refinement levels $\ell(i)$ of the substructures Ω_i.

We start the detailed description of the finite element space V^h by defining a multilevel triangulation within each substructure; see [20]. Each Ω_i is subdivided by a nested family of standard conforming finite element triangulations $\mathcal{T}_0^i = \{\Omega_i\}, \mathcal{T}_1^i, \mathcal{T}_2^i, \ldots, \mathcal{T}_{\ell(i)}^i$. The quasi-uniform triangulation $\mathcal{T}_{k+1}^i$ is obtained from the next coarser triangulation, $\mathcal{T}_k^i$, by subdividing each of its triangles into four, not necessarily equal, but shape-regular triangles. In particular, triangles of level $k+1$ have diameters of an order approximately one half of the diameter of those of level k.

2.2. The mortar finite elements. The interface Γ is defined by the coarse triangulation and is given by

$$\Gamma = \overline{\cup_{i=1}^I \partial\Omega_i \setminus \partial\Omega}.$$

A set of *mortars* $\{\gamma_m\}_{m=1}^M$ is obtained by selecting open edges of the substructures such that

$$\Gamma = \cup_{m=1}^M \overline{\gamma}_m, \quad \gamma_m \cap \gamma_n = \emptyset \ \text{ if } m \neq n.$$

Our view is that a mortar γ_m belongs to just one substructure, denoted by $\Omega_{i(m)}$, while the other edge, which geometrically occupies the same place, is denoted by δ_m. We refer to it as a *nonmortar*, and the subregion to which it belongs is denoted by $\Omega_{j(m)}$. The restrictions of the triangulations of $\Omega_{i(m)}$ and $\Omega_{j(m)}$ to this common edge will typically differ and are denoted by γ_m^h and δ_m^h, respectively. Discontinuous mortar finite element functions have different traces on γ_m and δ_m given by one-sided limits with respect to the two subregions $\Omega_{i(m)}$ and $\Omega_{j(m)}$. An important component of our preconditioner will be related to the union of the two subregions $\Omega_{i(m)}$ and $\Omega_{j(m)}$ and the edge in between, and we will denote this set by $\mathcal{R}(\gamma_m)$. Similarly, $\mathcal{R}(\Omega_i)$ is the union of all subregions Ω_j the closure of which intersects the closure of Ω_i. We also introduce the notation $V^h(\Sigma)$ to mean the restriction of V^h to a set Σ which, in this paper, will always be a single subregion or the union of a few of them. Finally, we denote by $V_0^h(\Sigma)$ the subspace of $V^h(\Sigma)$ of functions which vanish on $\partial\Sigma$.

Even though we will use a hierarchical basis in the design of our preconditioner, we can primarily work with a nodal basis. We will use a nodal basis of the mortar finite element space associated with the following sets of nodes:

- all nodes interior to the substructures and on $\partial\Omega_N$,
- all nodes interior to the mortars, and
- all nodes of vertices of subregions except those on $\partial\Omega_D$.

We denote by $\mathcal{V}$ the set of vertices of the substructures that are associated with degrees of freedom of V^h, i.e. those for which the values are not given by the Dirichlet data on $\partial\Omega_D$. Each crosspoint of Γ corresponds to several nodes of $\mathcal{V}$ and to one degree of freedom for each of the subregions that meet at that point; these nodes are in the same geometrical position, but are assigned to different subregions.

For each m, we further define a space of test functions $\mathcal{W}^h(\delta_m)$ given by the restriction to the nonmortar δ_m of the original finite element space defined on $\Omega_{j(m)}$ subject to the constraints that these continuous, piece-wise linear functions are constant in the first and last mesh intervals of δ_m^h.

The *mortar projection* π_m maps the space of finite element functions defined on γ_m^h into that of δ_m^h. Given $u^{i(m)}$ in $\Omega_{i(m)}$, and boundary values of $u^{j(m)}$ at the two endpoints v_{n_1} and v_{n_2} of δ_m, we determine the values of $\pi_m(u^{i(m)}, u^{j(m)}(v_{n_1}), u^{j(m)}(v_{n_2}))$ at the interior nodes of δ_m^h by

$$\int_{\delta_m} (u^{i(m)} - \pi_m(u^{i(m)}, u^{j(m)}(v_{n_1}), u^{j(m)}(v_{n_2}))\psi ds = 0 \quad \forall \psi \in \mathcal{W}^h(\delta_m). \tag{4}$$

After these preparations, the mortar finite element space V^h can now be fully defined. The restriction of V^h to Ω_i, $V^h(\Omega_i)$, is a regular conforming finite element space as described above. For each nonmortar there is a set of constraints,

$$u^{j(m)}|_{\delta_m} = \pi_m(u^{i(m)}, u^{j(m)}(v_{n_1}), u^{j(m)}(v_{n_2})), \tag{5}$$

which replace the pointwise continuity of conforming spaces.

The discrete problem is then:
Find $u \in V^h$ such that

$$a^\Gamma(u, v) = f^\Gamma(v) \quad \forall v \in V^h, \tag{6}$$

where $a^\Gamma(u, v)$ is defined in formula (1) and, similarly, $f^\Gamma(v)$ is the sum of contributions from the different subregions.

The rate of convergence of the solution of (6) to the solution of (3) is comparable to that of a conforming discretization; cf. [6], [8], and references therein for theoretical and experimental results.

At the expense of an exact solution of a finite element problem per subregion, with homogeneous Dirichlet data, we reduce problem (6) to that of finding the piece-wise discrete harmonic part of the solution. We recall that a finite element function u is discrete harmonic in the subregion Ω_i if

$$a^{\Gamma}(u,v) = 0 \quad \forall v \in V^h \cap H_0^1(\Omega_i),$$

and that a discrete harmonic function provides the unique minimal energy extension of finite element boundary data given on the boundary $\partial\Omega_i$. In what follows, we will work exclusively with piece-wise discrete harmonic functions, without restricting the generality of our discussion; from now on V^h will denote this subspace.

We next formulate a basic result proven in [8].

LEMMA 1. *The mapping π_m is stable:*

$$|\pi_m(u,0,0)|_{H_{00}^{1/2}(\delta_m)} \leq C|u|_{H_{00}^{1/2}(\gamma_m)} \quad \forall u \in H_{00}^{1/2}(\gamma_m). \tag{7}$$

We end the subsection by proving a Poincaré inequality and formulating a Friedrichs inequality. They will be formulated for a region $\mathcal{R}(c_r)$ which is the union of the substructures which have a crosspoint c_r in common. In order to obtain a result that is independent of the mesh, we will establish the inequality for a space $\hat{V}(\mathcal{R}(c_r))$, which contains all possible $V^h(\mathcal{R}(c_r))$ as a subspace but which itself is not a finite element space. The restriction of $\hat{V}(\mathcal{R}(c_r))$ to any of the substructures $\Omega_i \subset \mathcal{R}(c_r)$ equals $H^1(\Omega_i)$. As in the case of mortar finite element functions, we potentially have two traces on any edge Γ_{ij} between any pair of substructures Ω_i and Ω_j. We only impose one constraint per edge, namely that $\int_{\Gamma_{ij}}[u]ds = 0$, where $[u]$ is the jump of u across Γ_{ij}.

LEMMA 2. *Let $u \in \hat{V}(\mathcal{R}(c_r))$. Then,*

$$\inf_{c\in\Re} ||u-c||^2_{L^2(\mathcal{R}(c_r))} \leq C \sum_{\Omega_j \subset \mathcal{R}(c_r)} H_j^2 |u|^2_{H^1(\Omega_j)}. \tag{8}$$

Here C depends only on the minimal angle of the substructures that form the coarse triangulation of $\mathcal{R}(c_r)$ and is independent of the diameters of the substructures and their triangulations.

Proof. We note that we can confine our study to a finite number of configurations allowed by the minimal angle condition on the coarse mesh. Each configuration corresponds to a specific number of substructures that have the crosspoint c_r in common. We assume in our discussion that c_r is an interior crosspoint; the extension of our argument to cases when $c_r \in \partial\Omega_N$ poses no problems. The problem can be further specialized by noticing that a piece-wise affine map can be found that maps the triangulation of $\mathcal{R}(c_r)$ onto a regular polygon $\mathcal{R}(0)$ of diameter 1, centered at 0, the image of c_r. This mapping is benign under the assumption of shape regularity. It also accounts for the factors H_j^2 in the estimate.

Thus, what remains is to prove the Poincaré inequality (8) for this finite number of special reference regions. We use a variant of a well-known argument given, e.g. in Ciarlet [12, Theorem 3.1.1]. Our result follows by proving a bound

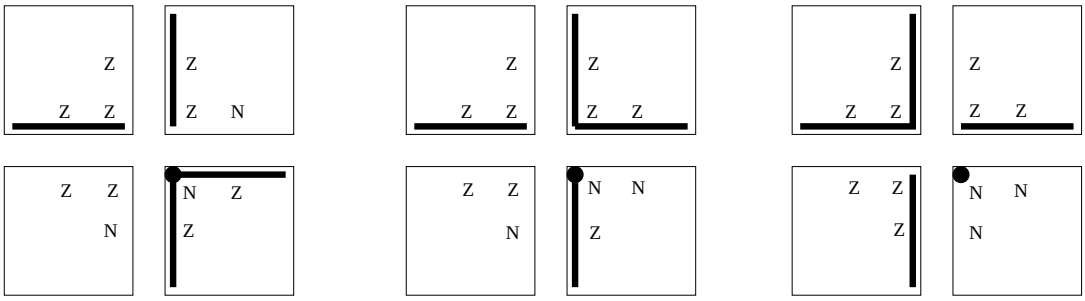

FIG. 1. *Three cases of vertex basis functions*

$$(9) \qquad \sum_{\Omega_j \subset \mathcal{R}(0)} \|u\|^2_{L^2(\Omega_j)} \leq C\Big(\sum_{\Omega_j \subset \mathcal{R}(0)} |u|^2_{H^1(\Omega_j)} + \Big(\int_{\mathcal{R}(0)} u(x)dx\Big)^2\Big) \quad \forall u \in \hat{V}(\mathcal{R}(0)).$$

Following Ciarlet, we use a proof by contradiction. We assume that there is a sequence of $u_k \in \hat{V}(\mathcal{R}(0))$ with unit L^2-norm, for which all the terms of the right hand side of (9) go to zero. By applying Rellich's theorem, one subregion at the time, selecting a subsequence of the previous subsequence every time we move on to a new subregion, we find a limit function which is locally in $H^1(\Omega_j)$, and which, because of the continuity of the trace mappings, satisfies the jump conditions of $\hat{V}(\mathcal{R}(0))$. Thus, the limit function belongs to $\hat{V}$, and is a constant, which must vanish since the last term of (9) vanishes in the limit. □

We note that a proof of the following Friedrichs inequality can be found in [7]; a proof can also be given using the same techniques as above.

LEMMA 3. *Let $u \in \hat{V}(\mathcal{R}(c_r))$ vanish on at least one of the edges of the substructures that form $\mathcal{R}(c_r)$. Then,*

$$(10) \qquad ||u||^2_{L^2(\mathcal{R}(c_r))} \leq C \sum_{\Omega_j \subset \mathcal{R}(c_r)} H_j^2 |u|^2_{H^1(\Omega_j)}.$$

Here C depends only on the minimal angle of the substructures that form the coarse triangulation of $\mathcal{R}(c_r)$ and is independent of the diameters of the substructures and their triangulations.

2.3. Vertex basis functions. As we have already pointed out, the mortar finite element functions are typically multi-valued at the crosspoints of the subregions. In order to describe and analyze our algorithm, we need to define a special vertex basis function for each of these degrees of freedom and derive estimates of their norms. These special functions are piece-wise discrete harmonic functions.

For each vertex v_n of $\mathcal{V}$, let $\phi_{v_n} \in V^h(\Omega)$ be defined by the value 1 at v_n, with all other nodal values on Γ set to zero. This completely defines ϕ_{v_n} since the interior nodal values on the nonmortars are given by the mortar projections, and those in the interior of the Ω_i by discrete harmonic extensions.

As indicated in Fig. 1, ϕ_{v_n} differs from zero at the interior nodes of some of the nonmortar edges associated with the same crosspoint as v_n. The marked node is the vertex v_n, and it touches two, one, or no mortars. In the figure, we distinguish between values at the vertices and at the interior nodes of the edges. The bold lines represent

mortars, and Z and N stand for zero and nonzero values of the vertex function ϕ_{v_n} at the vertices or at the interior nodes of the edges. The figure displays the three basic configurations in the case of four subregions meeting at a crosspoint.

In the first case, v_n is the left endpoint of a horizontal mortar γ_m. Then, ϕ_{v_n} coincides with the standard nodal basis function φ_{v_n} on γ_m. Across the edge, on the nonmortar, $\phi_{v_n}|_{\delta_m} = \pi_m(\varphi_{v_n}, 0, 0)$.

In the second and third cases, v_n is the left endpoint of a horizontal nonmortar δ_m. By construction, ϕ_{v_n} vanishes on the mortar γ_m across the edge. Therefore, $\phi_{v_n}|_{\delta_m} = \pi_m(0, 1, 0)$.

The following two lemmas provide estimates that will be used in Lemma 6 to estimate the $a^\Gamma(\cdot,\cdot)$- and L^∞-norms of ϕ_{v_n}.

LEMMA 4. *Let δ be a nonmortar and let π be the mortar projection associated with it. Then,*

$$||\pi(0,1,0)||_{L^\infty(\delta)} \leq C, \tag{11}$$

and

$$||\pi(0,1,0)||_{H^{1/2}(\delta)} \leq C. \tag{12}$$

Proof. Let $\underline{u}_\delta$ be the vector of nodal values, interior to δ, of $\pi(0,1,0)$. A nodal basis of $\mathcal{W}^h(\delta)$ is formed from the standard nodal basis on δ^h by combining two basis functions at each end to create two special basis functions which are constant in the mesh intervals of δ^h that touch the endpoints of δ^h.

By using (4), we obtain a tridiagonal system of linear equations

$$\mathcal{M}\underline{u}_\delta = \underline{b}.$$

It is easy to show that only the first and last diagonal elements of $\mathcal{M}$ differ from those of the mass matrix with respect to the space of piece-wise linear functions on δ^h that vanish at the endpoints. The differences between these matrix elements are positive and therefore

$$||\pi(0,1,0) - \varphi_{v_n}||^2_{L^2(\delta)} \leq \underline{u}_\delta^T \mathcal{M}\underline{u}_\delta \leq \underline{u}_\delta^T b \leq (\underline{u}_\delta^T \mathcal{M}\underline{u}_\delta)^{1/2}(\underline{b}^T\mathcal{M}^{-1}\underline{b})^{1/2},$$

where φ_{v_n} is the nodal basis function on δ^h associated with the left endpoint. By examining the right hand side $\underline{b}$, which has only one non-zero, we easily find, using the quasi-uniformity of δ^h, that

$$||\pi(0,1,0)||^2_{L^2(\delta)} \leq Ch_\delta,$$

from which (11) and (12) follow by using inverse inequalities. □

LEMMA 5. *Let v_n be the left endpoint of a mortar γ, and let φ_{v_n} be the standard nodal basis function on γ^h corresponding to v_n. Then,*

$$||\pi(\varphi_{v_n}, 0, 0)||_{L^\infty(\delta)} \leq C, \tag{13}$$

and

$$||\pi(\varphi_{v_n}, 0, 0)||_{H^{1/2}(\delta)} \leq C. \tag{14}$$

Proof. We first prove the lemma for $h_\delta \leq h_\gamma$; these are the minimal mesh sizes of δ^h and γ^h, respectively. In addition, we first also assume that the second leftmost point of γ^h, Q, coincides with a mesh point of δ^h. Using (4), we can easily check that

$$\pi(\varphi_{v_n}, 0, 0) - \varphi_{v_n} = -\pi(0, 1, 0),$$

since both sides are finite element functions on δ^h. The L^∞-norm estimate (13) now easily follows from (11). The $H^{1/2}$-norm estimate (14) is a consequence of $||\varphi_{v_n}||^2_{H^{1/2}} \leq C$ and (12).

If the second leftmost point of γ^h, Q, does not coincide with a mesh point of δ^h, we denote by R the mesh point of δ^h that is the right next neighbor of Q. Let $\tilde{\varphi}$ be the piece-wise linear function that equals 1 at v_n and vanishes at R, and to the right of R. Then, the argument just given can be used for $\tilde{\varphi}$, since it is now a finite element function on the mesh δ^h. There remains to estimate $\varphi_{v_n} - \tilde{\varphi}$. From the definition of $\tilde{\varphi}$, we find that $||\varphi_{v_n} - \tilde{\varphi}||^2_{L^2(\delta)} \leq Ch_\delta$. An argument similar to that of the proof of Lemma 4 shows that $||\pi(\varphi_{v_n} - \tilde{\varphi}, 0, 0)||^2_{L^2(\delta)} \leq Ch_\delta$, and we can conclude the proof of the result for $h_\delta \leq h_\gamma$ by using two inverse inequalities.

If $h_\delta > h_\gamma$, we can use that $||\varphi_{v_n}||_{L^2(\gamma)} \leq Ch_\gamma$ and an argument similar to that of the proof of Lemma 4, to conclude that

$$||\pi(\varphi_{v_n}, 0, 0)||_{L^2(\delta)} \leq Ch^2_\gamma / h_\delta \leq Ch_\gamma.$$

The two estimates (13) and (14) now follow as before. □

LEMMA 6. *For any $v_n \in \mathcal{V}$, we have:*

$$||\phi_{v_n}||_{L^\infty(\Gamma)} \leq C, \tag{15}$$

and

$$a^\Gamma(\phi_{v_n}, \phi_{v_n}) \leq C(1 + \ell). \tag{16}$$

Proof. The first bound, (15), follows immediately from Lemmas 4 and 5. The bound on the square of the trace norm, proportional to $(1 + \ell)$, follows from (15) and an argument in the proof of Lemma 3.2 in [19]. □

3. Algorithm and Analysis. Our solution procedure starts with the static condensation of all degrees of freedom interior to the different substructures, reducing the size of the discrete system. We note that it is not necessary to compute the Schur complement. All that is needed is to carry out a matrix-vector multiplication with the Schur complement. After finding sufficiently accurate values on Γ, the solution of (6) is then computed everywhere by solving a finite element problem for each subregion Ω_i with Dirichlet data given on $\partial\Omega_i \setminus \partial\Omega_N$.

3.1. Schwarz methods. We solve (6) with a preconditioned conjugate gradient method, using an additive Schwarz method determined by a finite family of subspaces $\{V_s\}$ whose sum spans V^h, and bilinear forms $\{b_s(\cdot,\cdot)\}_s$ defined on $V_s \times V_s$. Using the Schwarz framework described in Dryja and Widlund [14], we define approximate projections $T_s : V^h \to V_s$, by

$$b_s(T_s u, v_s) = a^\Gamma(u, v_s) \quad \forall v_s \in V_s.$$

The preconditioned operator T is given by

$$T = \alpha T_0 + \sum_{s \geq 1} T_s,$$

where α is a positive parameter that is used to tune the algorithm; see Section 4.

Let C_0^2 be a constant such that, for all $u \in V^h$, there exists $\{u_s\}_s$, $u_s \in V_s$, with

$$\sum_s b_s(u_s, u_s) \leq C_0^2 a^\Gamma(u,u) \quad \text{where} \quad u = \sum_s u_s,$$

and let ω be a constant such that

$$a^\Gamma(u,u) \leq \omega b_s(u,u) \quad \forall u \in V_s.$$

Since our algorithm is a two-level algorithm, the third hypothesis of Theorem 2.2 in [14] is trivially satisfied. This theorem then provides a bound on the condition number of T:

$$\kappa(T) \leq C C_0^2 \omega. \tag{17}$$

In subsection 3.3, we will introduce our algorithm and establish bounds for C_0 and ω.

3.2. A hierarchical basis. Before we can introduce our preconditioner in detail, we need to review some aspects of Yserentant's hierarchical basis method; cf. [20]. We denote by $\mathcal{N}_k^i$, $k = 0, 1, \ldots, \ell(i)$, the set of vertices of the triangles of $\mathcal{T}_k^i$, by V_k^i the space of continuous functions on $\overline{\Omega}_i$ that are linear in the triangles of $\mathcal{T}_k^i$, and by V^i the most refined space $V_{\ell(i)}^i$. All elements of V_k^i vanish on $\partial\Omega_i \cap \partial\Omega_D$. An interpolation operator $I_k^i : V^i \to V_k^i$, is defined by

$$I_k^i u(x) = u(x) \quad \forall x \in \mathcal{N}_k^i.$$

Following Yserentant [20], we define a discrete norm, for any set $\Lambda \subset \Omega_i$, by

$$|||u|||_\Lambda^2 = \sum_{k=1}^{\ell(i)} \sum_{x \in \mathcal{N}_k^i \setminus \mathcal{N}_{k-1}^i \cap \overline{\Lambda}} |(I_k^i u - I_{k-1}^i u)(x)|^2; \tag{18}$$

cf. Yserentant [20]. Let W_k^i be the image of $I_k^i - I_{k-1}^i$; this is the subspace of functions of V_k^i that vanish on $\mathcal{N}_{k-1}^i$. A hierarchical basis of V^i can now be defined recursively. The hierarchical basis of V_0^i is the standard finite element nodal basis restricted to the single triangle Ω_i. It is clear that $V_k^i = V_{k-1}^i + W_k^i$, $k \geq 1$. In each step, we augment the hierarchical basis of V_{k-1}^i by the level k nodal basis functions which span $W_k^i \subset V_k^i$. For a function u represented in this basis, the discrete norm $|||u|||_\Lambda^2$ is simply the Euclidean norm and thus very easy to compute. Moreover, the transformation between the standard nodal basis and the hierarchical basis is very fast and easy to implement; see [18] and [20].

We first describe some results that have motivated the definition of our preconditioner. For one substructure, we have:

$$|I_0^i u|_{H^1(\Omega_i)}^2 + |||u|||_{\Omega_i}^2 \leq C(1 + \ell(i)) ||u||_{L^\infty(\Omega_i)}^2 \quad \forall u \in V^i, \tag{19}$$

and

$$|u|^2_{H^1(\Omega_i)} \leq C(|I^i_0 u|^2_{H^1(\Omega_i)} + |||u|||^2_{\Omega_i}) \quad \forall u \in V^i. \tag{20}$$

Equation (19) is an easy consequence of the definition of the interpolation operators. Equation (20) results from a strengthened Cauchy-Schwarz inequality; see Yserentant [20].

For our purposes, we need a variant of (20):

LEMMA 7. *For $u \in V^h(\Omega_i)$,*

$$|u|^2_{H^1(\Omega_i)} \leq C(|I^i_0 u|^2_{H^1(\Omega_i)} + |||u|||^2_{\partial\Omega_i}). \tag{21}$$

Proof. We first define an extension $E(u) \in V^i$ of u, normally not discrete harmonic, such that $E(u)$ agrees with u on $\partial\Omega_i$, and when written in the hierarchical representation, has all its degrees of freedom in the open set Ω_i equal to zero. Equation (20), applied to $E(u)$, implies

$$|E(u)|^2_{H^1(\Omega_i)} \leq C(|I^i_0 u|^2_{H^1(\Omega_i)} + |||u|||^2_{\partial\Omega_i}),$$

since $|||E(u)|||_{\Omega_i} = |||u|||_{\partial\Omega_i}$. We conclude by noting that the discrete harmonic function u has the smallest energy among all extensions in V^i of the boundary values of u. □

3.3. The algorithm. We are now in a position to describe and analyze our algorithm. The coarse space, which is conforming, is given by

$$V_0 = \{u \in V^h \cap H^1_0(\Omega, \partial\Omega_D) |\ u \text{ is linear on each } \Omega_i\}.$$

The bilinear form associated with V_0 is $a^\Gamma(\cdot,\cdot)$ which coincides with $a(\cdot,\cdot)$ on this subspace.

A one-dimensional vertex space is associated with each $v_n \in \mathcal{V}$:

$$V_{v_n} = \text{span of } \phi_{v_n}.$$

We use the exact bilinear form $a^\Gamma(\cdot,\cdot)$ for these spaces.

A subspace $V_{\gamma_m} = V^h_0(\mathcal{R}(\gamma_m))$ is associated with each mortar. The bilinear forms for these spaces are given by $b_{\gamma_m}(\cdot,\cdot) = |||\cdot|||^2_{\gamma_m}$.

The Schwarz framework provides a preconditioned equation $Tu = b$ in terms of these spaces and bilinear forms and the solution of this equation is the same as that of (6). The main result of this paper is the following theorem. We note that a more straightforward approach to the proof would lead to a bound with a fourth power of ℓ.

THEOREM 1. *The condition number of T satisfies*

$$\kappa(T) \leq C(1+\ell)^2.$$

Proof. We first partition $u \in V^h$ and obtain the estimate $C_0^2 \leq C(1+\ell)^2$. To do so, we select $u_0 \in V_0$, in the representation of $u = \sum u_s$, by making $u_0(c_r) = \bar{u}_{c_r}$, where $\bar{u}_{c_r}$ is the average value of u at the vertices of $\mathcal{V}$ that coincide geometrically with c_r. A standard Sobolev-like inequality for finite elements, see e.g. [10], gives:

$$\begin{aligned} |u(v_n) - u_0(v_n)|^2 &\leq C \sum_{\Omega_j \subset \mathcal{R}(c_r)} (1 + \log(H_j/h_j))(|u|^2_{H^1(\Omega_j)} + \frac{1}{H_j^2}||u||^2_{L^2(\Omega_j)}) \\ &\leq C(1+\ell) \sum_{\Omega_j \subset \mathcal{R}(c_r)} (|u|^2_{H^1(\Omega_j)} + \frac{1}{H_j^2}||u||^2_{L^2(\Omega_j)}), \end{aligned} \tag{22}$$

since $\log(H_j/h_j)$ is proportional to $\ell(j)$.

If $\mathcal{R}(c_r)$ has a whole edge on $\partial\Omega_D$, then the last sum above can be bounded by $a^\Gamma_{\mathcal{R}(c_r)}(u,u)$, the restriction of $a^\Gamma(\cdot,\cdot)$ to $\mathcal{R}(c_r)$, by using Lemma 3. If $\mathcal{R}(c_r)$ has only one point in common with $\partial\Omega_D$, we consider its union with an additional subregion, chosen so that this new $\mathcal{R}(c_r)$ has a whole edge on $\partial\Omega_D$, and use Lemma 3 again. If $\partial\Omega_i \cap \partial\Omega_D = \emptyset$, we add a constant to u, which does not change the left hand side, and use Lemma 2. For any of these three cases, we have:

$$|u(v_n) - u_0(v_n)|^2 \leq C(1+\ell) \sum_{\Omega_j \subset \mathcal{R}(c_r)} |u|^2_{H^1(\Omega_j)}, \tag{23}$$

which in turn implies, by a standard argument, that

$$|u_0|^2_{H^1(\Omega_i)} \leq C(1+\ell) \sum_{\Omega_j \subset \mathcal{R}(c_r)} |u|^2_{H^1(\Omega_j)}. \tag{24}$$

We next define the vertex space components of u. For each vertex $v_n \in \mathcal{V}$, let $u_{v_n} = (u-u_0)(v_n)\phi_{v_n}$. Using equation (16) and (23), we obtain

$$\begin{aligned} a^\Gamma(u_{v_n}, u_{v_n}) &\leq C(1+\ell)|(u-u_0)(v_n)|^2 \\ &\leq C(1+\ell)^2 a^\Gamma_{\mathcal{R}(c_r)}(u,u), \end{aligned} \tag{25}$$

where c_r is the crosspoint that coincides geometrically with v_n.

Let $w = u - u_0 - \sum_{v_n} u_{v_n}$. Then, w vanishes at all the vertices. For each mortar γ_m, let $u_{\gamma_m} \in V_{\gamma_m}$ coincide with w on γ_m. It is easy to see that $u = u_0 + \sum_n u_{v_n} + \sum_m u_{\gamma_m}$, and that

$$\sum_{m=1}^{M} |||u_{\gamma_m}|||^2_{\gamma_m} \leq \sum_{i=1}^{I} |||w|||^2_{\partial\Omega_i}.$$

By the argument used to derive (19), we have

$$|||w|||^2_{\partial\Omega_i} \leq C(1+\ell)\|w\|^2_{L^\infty(\partial\Omega_i)}.$$

By (15), we know that $\|\phi_{v_n}\|_{L^\infty(\Gamma)} \leq C$ for all $v_n \in \mathcal{V}$. Hence,

$$\begin{aligned} |||w|||^2_{\partial\Omega_i} &\leq C(1+\ell)||u-u_0||^2_{L^\infty(\partial\Omega_i)} \\ &\leq C(1+\ell)(||u||^2_{L^\infty(\Omega_i)} + \sum_{c_r \in \Omega_i} |u_0(c_r)|^2) \\ &\leq C(1+\ell)^2 (\sum_{\Omega_j \subset \mathcal{R}(\Omega_i)} |u|^2_{H^1(\Omega_j)} + \frac{1}{H_j^2}||u||^2_{L^2(\Omega_j)}), \end{aligned}$$

since the value of u_0 at c_r depends only on the values of u at the vertices that coincide geometrically with c_r, and by using the same Sobolev-like inequality used to derive (22).

We now repeat the quotient space argument of (23), and obtain

$$|||w|||^2_{\partial\Omega_i} \leq C(1+\ell)^2 a^\Gamma_{\mathcal{R}(\Omega_i)}(u,u).$$

Summing over all subregions, we find

$$\sum_{m=1}^{M} |||u_{\gamma_m}|||^2_{\gamma_m} \leq C(1+\ell)^2 \sum_{i=1}^{I} a^\Gamma_{\mathcal{R}(\Omega_i)}(u,u). \tag{26}$$

Every point of Ω is covered only a small number of times by $\{\mathcal{R}(c_r)\}$, c_r a cross-point, and by $\{\mathcal{R}(\Omega_i)\}$. We use (24), sum (25) over all c_r, and (26) to obtain

$$|u_0|^2_{H^1(\Omega)} \quad + \sum_{v_n \in \mathcal{V}} a^\Gamma(u_{x_n}, u_{x_n}) + \sum_{m=1}^M |||u_{\gamma_m}|||^2_{\gamma_m} \\ \leq C(1+\ell)^2 a^\Gamma(u,u),$$

which completes the estimate of C_0^2.

Our next task is to show that ω can be bounded by a constant. Fortunately, this is a very simple matter. For the coarse and vertex spaces, $\omega = 1$, since we use exact solvers for these spaces. Let $u \in V_{\gamma_m}$. Then,

$$a^\Gamma(u,u) = |u|^2_{H^1(\Omega_{i(m)})} + |u|^2_{H^1(\Omega_{j(m)})}.$$

The stability of the mortar projection, Lemma 1, the standard trace theorem, and an extension theorem for finite element functions, [9, Lemma 5.1], allow us to bound the second term of the right hand side by the first. Then (21) can be used to obtain

$$a^\Gamma(u,u) \leq C|||u|||^2_{\gamma_m} = C b_{\gamma_m}(u,u) \quad \forall u \in V_{\gamma_m},$$

since the elements of V_{γ_m} vanish at the subdomain vertices. Hence, $\omega \leq C$. □

4. Numerical Experiments. Our method has been implemented in MATLAB, and the code is general enough to treat regions that can be decomposed into the union of rectangles aligned with the axes; the mesh inside each subregion can be any tensor product mesh, and the meshes do not necessarily match on the interface between the subregions. We only report results for a very simple region; we note that even for more general ones, the algorithm appears to be insensitive to quite different mesh sizes in adjacent regions.

In a first set of experiments, the region Ω is the unit square, divided uniformly into $M \times M$ substructures, where M is 2, 4, 8, or 16. The substructures are squares, and V_0 is the space of continuous, piece-wise bilinear functions on the coarse triangulation. For every $N \in \{4, 8, 16, 32\}$, each substructure is divided into an $N \times (N+4)$ grid of smaller rectangles, if the substructure is in an odd row, and into an $(N+4) \times N$ grid if it is in an even row. These small rectangles are then divided into two triangles by drawing the diagonals from bottom left to top right. The meshes do not match at the interfaces of the substructures; we assign mortars and nonmortars in an arbitrary fashion. The results are summarized on Table 1, which is organized in the same way as Table 2 in [18] to facilitate a comparison. The number of refinement levels is approximately equal to $\log_2(MN)$ starting from the entire region.

In a second set of experiments, odd rows of subregions have uniform grids of $N \times N$ squares divided into two triangles each, and even lines have $(N+4) \times (N+4)$ squares also divided in two triangles each. Table 2 summarizes the results for this case.

As in [18], the coarse space V_0 generates a separate contribution to the preconditioner, which may be multiplied by a constant α in order to improve the overall condition number; cf. Subsection 3.1. In our experiments, we found that $\alpha = 5$ is close to the optimal parameter value for a large range of N and M, and all the results reported have been obtained with this value of α.

We remark that the growth of the condition number is virtually independent of M^2, the number of substructures, if we fix the value of $H/h = N$. Our results are quantitatively slightly better than the results obtained in the conforming case. This appears to

TABLE 1

Condition numbers for the $N \times (N+4)$ case

Refinement levels	3	4	5	6	7	8	9
N	4	8	16	32			
M=2	7.84	7.26	8.30	10.11			
N		4	8	16	32		
M=4		9.95	8.24	8.58	10.35		
N			4	8	16	32	
M=8			10.01	8.22	8.88	11.23	
N				4	8	16	32
M=16				10.94	8.27	9.09	N/A

TABLE 2

Condition numbers for the $N \times N$ and $(N+4) \times (N+4)$ case

Refinement levels	3	4	5	6	7	8	9
N	4	8	16	32			
M=2	5.48	6.32	7.80	9.81			
N		4	8	16	32		
M=4		9.30	7.95	8.36	10.28		
N			4	8	16	32	
M=8			9.46	8.36	9.01	11.23	
N				4	8	16	32
M=16				9.52	8.55	9.21	11.48

be due to a larger overlap of the subspaces in a neighborhood of the crosspoints, since several subspaces are nonzero there. It can also be an effect of using parameters, different from those of the conforming case, to scale the contribution of the coarse problem to the preconditioner.

The growth is also consistent with the estimate $\log^2(N)$ given by Theorem 1. For small values of N, N and $N+4$ differ substantially, and this appears to be the reason for the variations in this pattern found in the tables.

REFERENCES

[1] Y. Achdou and Y. A. Kuznetsov, *Substructuring preconditioners for finite element methods on nonmatching grids*, East-West J. Numer. Math., 3 (1995), pp. 1–28.

[2] Y. Achdou, Y. A. Kuznetsov, and O. Pironneau, *Substructuring preconditioners for the Q_1 mortar element method*, Numer. Math., 71 (1995), pp. 419–449.

[3] Y. Achdou, Y. Maday, and O. B. Widlund, *Méthode itérative de sous-structuration pour les éléments avec joints*, tech. rep., Analyse Numérique-CNRS et Université Pierre et Marie Curie, Paris, France, October 1995. Note submitted to C.R. Acad. Sci. Paris.

[4] F. Ben Belgacem, *Discretisations 3D Non Conformes pour la Méthode de Decomposition de Domaine des Elément avec Joints: Analyse Mathématique et Mise en Œvre pour le Probleme de Poisson*, PhD thesis, Université Pierre et Marie Curie, Paris, France, January 1993. Tech. Rep. HI-72/93017, Electricité de France.

[5] F. Ben Belgacem and Y. Maday, *Adaption de la méthode des éléments avec joints au couplage spectral élments finis en dimension 3: étude de l'érreur pour l'équation de Poisson*, tech. rep., Electricité de France, April 1992. Tech. Rep. HI-72/7095.

[6] ———, *The mortar element method for three dimensional finite elements.* Unpublished paper based on Yvon Maday's talk at the Seventh International Conference of Domain Decomposition Methods in Scientific and Engineering Computing, held at Penn State University, October 27-30, 1993.

[7] C. Bernardi and Y. Maday, *Mesh adaptivity in finite elements by the mortar method*, Tech. Rep. R94029, Laboratoire d'Analyse Numérique, Université Pierre et Marie Curie – Centre National de la Recherche Scientifique, January 1995.

[8] C. Bernardi, Y. Maday, and A. T. Patera, *A new non conforming approach to domain decomposition: The mortar element method*, in Collège de France Seminar, H. Brezis and J.-L. Lions, eds., Pitman, 1994. This paper appeared as a technical report about five years earlier.

[9] P. E. Bjørstad and O. B. Widlund, *Iterative methods for the solution of elliptic problems on regions partitioned into substructures*, SIAM J. Numer. Anal., 23 (1986), pp. 1093–1120.

[10] J. H. Bramble, *A second order finite difference analogue of the first biharmonic boundary value problem*, Numer. Math., 9 (1966), pp. 236–249.

[11] M. A. Casarin, *Diagonal edge preconditioners in p-version and spectral element methods*, Tech. Rep. 704, Department of Computer Science, Courant Institute, September 1995.

[12] P. G. Ciarlet, *The Finite Element Method for Elliptic Problems*, North-Holland, Amsterdam, 1978.

[13] M. Dryja, *Additive Schwarz methods for elliptic mortar finite element problems*, in Modeling and Optimization of Distributed Parameter Systems with Applications to Engineering, K. Malanowski, Z. Nahorski, and M. Peszynska, eds., IFIP, Chapman & Hall, London, 1996. To appear.

[14] M. Dryja and O. B. Widlund, *Schwarz methods of Neumann-Neumann type for three-dimensional elliptic finite element problems*, Comm. Pure Appl. Math., 48 (1995), pp. 121–155.

[15] P. Le Tallec, *Neumann-Neumann domain decomposition algorithms for solving 2D elliptic problems with nonmatching grids*, East-West J. Numer. Math., 1 (1993), pp. 129–146.

[16] Y. Maday and O. B. Widlund, *Some iterative substructuring methods for mortar finite elements: The lower order case*, tech. rep., Courant Institute of Mathematical Sciences, 1995. In preparation.

[17] B. F. Smith, *Domain Decomposition Algorithms for the Partial Differential Equations of Linear Elasticity*, PhD thesis, Courant Institute of Mathematical Sciences, September 1990. Tech. Rep. 517, Department of Computer Science, Courant Institute.

[18] B. F. Smith and O. B. Widlund, *A domain decomposition algorithm using a hierarchical basis*, SIAM J. Sci. Stat. Comput., 11 (1990), pp. 1212–1220.

[19] O. B. Widlund, *Iterative substructuring methods: Algorithms and theory for elliptic problems in the plane*, in First International Symposium on Domain Decomposition Methods for Partial Differential Equations, R. Glowinski, G. H. Golub, G. A. Meurant, and J. Périaux, eds., Philadelphia, PA, 1988, SIAM.

[20] H. Yserentant, *On the multi-level splitting of finite element spaces*, Numer. Math., 49 (1986), pp. 379–412.